기초과학연구

목 차

통계학

수학

전자물리학

J. Basic Sci., HUFS, **61** (2026), pp. 1-7

Data-Sharpened Cross-Validation for Nonparametric Regression[1]

Kee-Hoon Kang[2]

ABSTRACT. Cross-validation is a standard tool for selecting smoothing parameters in nonparametric regression. Despite its wide applicability, conventional cross-validation often suffers from high variability and limited bias reduction. In this paper, we revisit a data-sharpened cross-validation (DSCV) approach in which not only the smoothing parameter but also the observed response values are adjusted through the cross-validation criterion. While the original formulation emphasized theoretical improvements and density estimation, this study focuses on nonparametric regression and practical performance. Through simulation studies based on local linear regression, we demonstrate that DSCV consistently improves mean integrated squared error relative to conventional cross-validation and popular plug-in methods. The results suggest that data-sharpened cross-validation provides a simple and effective bias–variance trade-off improvement for regression problems.

Introduction

Cross-validation plays a central role in smoothing parameter selection for nonparametric curve estimation. In regression settings, it is particularly attractive because it requires minimal assumptions and avoids the need for pilot smoothing parameters. For these reasons, cross-validation has become the default method for bandwidth selection in kernel and local polynomial regression. Nevertheless, it is well known that cross-validation bandwidths can be highly variable, especially in small or moderate samples. This variability often results in undersmoothing, leading to regression estimates with unnecessary roughness.

While undersmoothing may preserve local features, it increases variance and may degrade overall estimation accuracy. A complementary line of research has focused on data sharpening**,** where observed data are slightly modified prior to estimation in order to reduce bias. Data sharpening methods have been proposed for both density estimation and regression, typically as plug-in bias correction techniques. However, these approaches tend to be problem-specific

---

[1] This research was supported by the research fund 2025 of Hankuk University of Foreign Studies.
[2] Department of Statistics, Hankuk University of Foreign Studies, Yongin 17035, Republic of Korea. E-mail: khkang@hufs.ac.kr

and often rely on higher-order asymptotic approximations.

The key idea explored in this paper is that cross-validation itself can be used to determine how the data should be sharpened. The idea of allowing cross-validation to alter not only the smoothing parameter but also the data themselves was formalized by Hall and Kang (2005), who showed that such an approach can improve the order of mean squared error under suitable constraints. Instead of treating the observed data as fixed inputs, we allow them to vary within the cross-validation criterion, subject to mild constraints. This leads to data-sharpened cross-validation (DSCV), a unified and automatic procedure that simultaneously selects the smoothing parameter and adjusts the data.

While the original formulation of DSCV addressed both density estimation and regression with substantial theoretical development, the present paper focuses on nonparametric regression, emphasizing practical implementation and finite-sample performance. Our goal is to provide an application-oriented account suitable for applied researchers. A complementary line of research has focused on data sharpening, in which observed data are slightly adjusted prior to estimation in order to reduce bias. Early developments of this idea were proposed in the context of density estimation and nonparametric regression, demonstrating that modest data perturbations can lead to meaningful bias reduction (Choi and Hall, 2000; Choi et al., 2000).

Data-Sharpened Cross-Validation for Regression

Regression framework

Let $(U_i, V_i), i = 1, \dots, n$ be independent observations generated from the regression model

$$V_i = g(U_i) + \varepsilon_i,$$

where $g(\cdot)$ is an unknown smooth regression function and the errors satisfy $E(\varepsilon_i | U_i) = 0$. Consider a linear nonparametric regression estimator of the form

$$\hat{g}(x) = \sum_{j=1}^{n} V_j \, w_j(x; h),$$

where $w_j(x; h)$ are weights depending on the design points $U_1, \ldots, U_n$ and a smoothing parameter h. Local linear regression is a canonical example of this framework. Unlike conventional plug-in bias correction techniques, which are often problem-specific and rely on higher-order derivative estimation, data-sharpened cross-validation provides a unified and automatic framework applicable across a wide range of smoothing problems (Fan and Gijbels, 1996; Loader, 1999).

Standard leave-one-out cross-validation selects h by minimizing

$$\mathrm{CV}(h) = \frac{1}{n}\sum_{i=1}^{n}\{V_i - \hat{g}_{-i}(U_i; \mathrm{h})\}^2$$

where $\hat{g}_{-i}$ denotes the estimator computed with the *i*th observation removed.

Data sharpening via cross-validation

In data-sharpened cross-validation, we introduce adjusted response values $Y_1, \ldots, Y_n$ while keeping the covariates Y_i fixed. Let

$$\hat{g}_Y(x) = \sum_{j=1}^{n} Y_j \, w_j(x; h)$$

be the regression estimator computed from the sharpened responses.

The DSCV criterion is defined as

$$CV(Y, h) = \frac{1}{n}\sum_{i=1}^{n}\{V_i - \hat{g}_{Y,-i}(U_i; h)\}^2,$$

where $\hat{g}_{Y,-i}$ is obtained from $\{(U_j, Y_j): j \neq i\}$.

Crucially, the observed responses V_i are used only in the evaluation of prediction error, while the adjusted values Y_j enter the regression estimator. The pair (Y, h) is chosen to minimize $\mathrm{CV(Y, h)}$, subject to constraints of the form

$$|Y_i - V_i| \leq rh, \;\; i = 1, \ldots, n,$$

where $r > 0$ controls the extent of allowable data movement.

This formulation preserves the interpretability of cross-validation while introducing additional flexibility to reduce bias. The final regression estimator is $\hat{g}_{Y^*}$, where (Y^*, h^*) minimizes the constrained DSCV criterion.

Simulation Design

We investigate the finite-sample performance of DSCV using local linear regression in two standard regression settings:

$$\text{(Model 1)} \quad V = cos(2\pi U) + \epsilon,$$

$$\text{(Model 2)} \quad V = U + 3exp(-2U^2) + \epsilon,$$

where $U \sim Uniform(0,1)$ and $\epsilon \sim N(0, 0.1^2)$.

Sample sizes $n = 40, 60, 100$ were considered, with 500 Monte Carlo replications per setting. Performance was evaluated using mean integrated squared error (MISE), approximated numerically over a fine grid.

DSCV was compared with:

- standard leave-one-out cross-validation (LSCV),
- a plug-in bandwidth selector for local linear regression.

Results and Discussion

Across all models and sample sizes, DSCV consistently outperformed both LSCV and plug-in methods. The improvement in MISE typically ranged from 5% to 12%, with larger gains observed for smaller sample sizes and more nonlinear regression functions. An important practical observation is that DSCV often selected slightly larger bandwidths than standard cross-validation, compensating for this increased smoothing through data sharpening. As a result, DSCV estimates exhibited reduced variance without introducing excessive bias. Sensitivity analysis with respect to the constraint parameter r showed that moderate values yielded stable improvements, while excessively large values provided little additional benefit.

Recent studies have further demonstrated that data sharpening can be effectively combined with additional structural considerations, such as shape constraints or dependent data settings, leading to improved finite-sample performance in regression and related problems (Braun et al., 2018; Snyman et al., 2021).

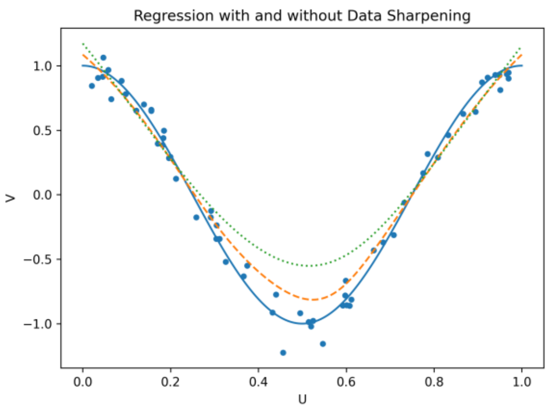

Figure 1. Local linear regression estimates with and without data sharpening. The solid curve represents the true regression function $g(x) = \cos(2\pi x)$. The dotted curve corresponds to the standard cross-validation estimator, while the dashed curve shows the data-sharpened cross-validation (DSCV) estimator.

The simulation results confirm that data-sharpened cross-validation offers a practical improvement over conventional bandwidth selection methods in nonparametric regression. Unlike plug-in bias correction techniques, DSCV does not require explicit estimation of higher-order derivatives or problem-specific adjustments. From an applied perspective, DSCV has several appealing features:

1. It retains the familiar structure of cross-validation.
2. It automatically balances bias and variance through joint optimization.
3. It can be implemented with standard numerical optimization routines.

The main limitation is increased computational cost due to the higher-dimensional optimization. However, with modern computing resources and moderate sample sizes typical of applied regression problems, this cost remains manageable.

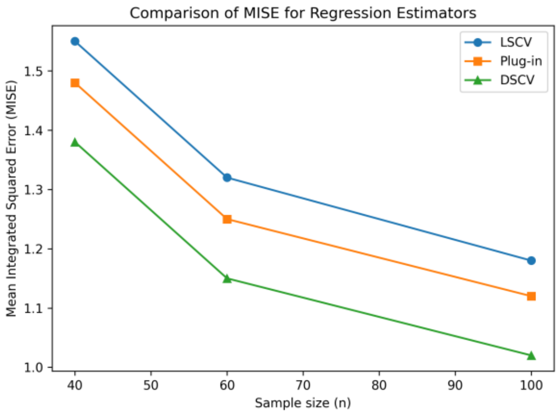

Figure 2. Mean integrated squared error (MISE) comparison for nonparametric regression estimators. The data-sharpened cross-validation (DSCV) estimator consistently outperforms standard cross-validation (LSCV) and plug-in bandwidth selection across all sample sizes.

Conclusion

This paper revisits data-sharpened cross-validation from an application-oriented perspective, focusing on nonparametric regression. By allowing response values to be adjusted within the cross-validation framework, DSCV achieves consistent finite-sample improvements in estimation accuracy.

Given its generality and ease of interpretation, DSCV provides a useful alternative to conventional bandwidth selection methods, particularly in settings where bias reduction is important and sample sizes are limited. Future work may explore extensions to shape-constrained regression, dependent data, and high-dimensional smoothing problems.

These recent extensions suggest that data-sharpened cross-validation may serve as a useful building block for more complex smoothing frameworks, including shape-constrained regression and dependent data models, while retaining the interpretability and flexibility of classical cross-validation methods.

Acknowledgements
이 연구는 2025년 한국외국어대학교 학술연구비 지원에 의해 이루어진 것임.

References

[1] Braun, W. J., Hall, P. and Titterington, D. M. (2018). Data sharpening for smoothing under shape constraints. *Journal of Computational and Graphical Statistics*, 27, 697–707.

[2] Choi, E. and Hall, P. (2000). Data sharpening as a prelude to density estimation. *Biometrika*, 87, 941–947.

[3] Choi, E., Hall, P. and Rousson, V. (2000). Data sharpening methods for bias reduction in nonparametric regression. *Annals of Statistics*, 28, 133–151.

[4] Fan, J. and Gijbels, I. (1996). *Local Polynomial Modelling and Its Applications*. Chapman & Hall.

[5] Loader, C. (1999). *Local Regression and Likelihood*. Springer.

[6] Park, B.U. and Marron, J.S. (1990). Comparison of data-driven bandwidth selectors. *Journal of the American Statistical Association*, 85, 66−72.

[7] Sheather, S.J. and Jones, M.C. (1991). A reliable data-based bandwidth selection method. *Journal of the Royal Statistical Society, Series B*, 53, 683–690.

저자정보

주저자: 강기훈 / 한국외국어대학교 통계학과 / 교수

J. Basic Sci. HUFS **61** (2026), pp. 8–18

INVERSE LIMITS OF CM POINTS ON SOME MODULAR CURVES

DONG HWA SHIN

Abstract. Let K be an imaginary quadratic field with discriminant d_K. For a positive integer N, let $\mathcal{CM}_0(d_K,\,N)^{\pm}$ denote the subset of the Shimura variety $Y_0(N)^{\pm}$ consisting of CM points of discriminant d_K which are primitive modulo N. We show that the inverse limit

$$\varprojlim_N \mathcal{CM}_0(d_K,\,N)^{\pm} \text{ in } \varprojlim_N Y_0(N)^{\pm}$$

admits a natural group structure which is isomorphic to the Galois group $\mathrm{Gal}(K^{\mathrm{ring}}/\mathbb{Q})$, where K^{ring} is the compositum of all ring class fields of K.

1. Introduction

Let K be an imaginary quadratic field with ring of integers $\mathcal{O}_K$. Let N be a positive integer, and let $\mathcal{O}=\mathcal{O}_N$ be the order in K of conductor N. By the existence theorem of class field theory (see [1, §8–9], [5, Chapter V] or [11, Chapter IV]), there is a unique abelian extension $H_\mathcal{O}$ of K such that

(i) every prime ideal of K ramified in $H_\mathcal{O}$ divides $N\mathcal{O}_K$,
(ii) the Galois group $\mathrm{Gal}(H_\mathcal{O}/K)$ is isomorphic to the $\mathcal{O}$-ideal class group
$$\mathcal{C}(\mathcal{O}):=I(\mathcal{O})/P(\mathcal{O})$$
via the Artin map of modulus $N\mathcal{O}_K$, where $I(\mathcal{O})$ is the group of proper fractional $\mathcal{O}$-ideals and $P(\mathcal{O})$ is its subgroup consisting of principal fractional $\mathcal{O}$-ideals.

The field $H_\mathcal{O}$ is called the *ring class field* of the order $\mathcal{O}$ in K. Specifically, if $N=1$, then $H_\mathcal{O}$ is nothing but the Hilbert class field of K, which is the maximal unramified abelian extension of K (see [1, Theorem 8.10]). As a

2020 *Mathematics Subject Classification.* Primary 11R37; Secondary 11E57, 11G18.
THIS WORK WAS SUPPORTED BY HANKUK UNIVERSITY OF FOREIGN STUDIES RESEARCH FUND OF 2025.

consequence of the theory of complex multiplication (on elliptic curves), established by Hasse [2], Deuring [3], etc., we have

$$H_{\mathcal{O}} = K(j(\mathcal{O}))$$

where $j(\mathcal{O})$ is the invariant of the elliptic curve isomorphic to $\mathbb{C}/\mathcal{O}$.

On the other hand, for a negative integer D such that $D \equiv 0$ or $1 \pmod 4$, Gauss [4] introduced the form class group $\mathcal{C}(D)$ of discriminant D, which is a prototype of a finite abelian group. Later, essentially due to Dedekind, it was shown that

$$\mathcal{C}(D) \simeq \mathcal{C}(\mathcal{O})$$

if D is the discriminant of an order $\mathcal{O}$ in K. More precisely, let $\mathcal{Q}(D)$ $(\subset \mathbb{Z}[x,\, y])$ be the set of primitive positive definite binary quadratic forms over $\mathbb{Z}$. For $Q(x,\, y) = ax^2 + bxy + cy^2 \in \mathcal{Q}(D)$, let ω_Q denote the zero of the quadratic polynomial $Q(x,\, 1)$ lying in the complex upper half-plane $\mathbb{H} = \{\tau \in \mathbb{C} \mid \mathrm{Im}(\tau) > 0\}$, namely,

$$\omega_Q := \frac{-b + \sqrt{D}}{2a}. \tag{1}$$

For $\xi_1,\, \xi_2 \in \mathbb{C}$ which are linearly independent over $\mathbb{R}$, write $[\xi_1,\, \xi_2]$ for the lattice in $\mathbb{C}$ generated by $\xi_1,\, \xi_2$ over $\mathbb{Z}$, that is,

$$[\xi_1,\, \xi_2] := \mathbb{Z}\xi_1 + \mathbb{Z}\xi_2.$$

Then the map

$$\begin{aligned} \mathcal{C}(D) &\to \mathcal{C}(\mathcal{O}) \\ [Q] &\mapsto [[\omega_Q,\, 1]] = [[(-b + \sqrt{D})/2,\, a]] \end{aligned}$$

is a well-defined isomorphism (see [1, Theorem 7.7]).

Let $\Gamma_0(N)$ be the Hecke congruence subgroup (of $\mathrm{SL}_2(\mathbb{Z})$) of level N, given by

$$\Gamma_0(N) := \left\{ \gamma \in \mathrm{SL}_2(\mathbb{Z}) \mid \gamma \equiv \begin{bmatrix} * & * \\ 0 & * \end{bmatrix} \pmod N \right\}.$$

Let

$$Y_0(N) := \Gamma_0(N)\backslash\mathbb{H} \quad \text{and} \quad Y_0(N)^- := \Gamma_0(N)\backslash\mathbb{H}^-$$

be the associated (open) modular curves, where $\mathbb{H}^-$ is the complex lower half-plane. The aim of this paper is to provide a concrete realization of class field theory for imaginary quadratic fields in terms of the inverse limits of CM points (see Definitions 4.1 and 4.2) on the Shimura varieties

$$Y_0(N)^\pm := Y_0(N) \sqcup Y_0(N)^- \quad (N \geq 1).$$

The main result of this paper is the following.

Theorem A (Theorem 4.4)**.** *Let K be an imaginary quadratic field. Then the inverse limit*

$$\varprojlim_N \mathcal{CM}_0(d_K,\, N)^\pm \quad (\subset \varprojlim_N Y_0(N)^\pm)$$

can be regarded as a group isomorphic to the Galois group $\mathrm{Gal}(K^{\mathrm{ring}}/\mathbb{Q})$*, where K^{ring} denotes the compositum of all ring class fields $H_{\mathcal{O}_N}$.*

Throughout this paper, we use the following notation:

- K : an imaginary quadratic field,
- d_K : the discriminant of K,
- $\mathcal{O}_K$: the ring of integers of K,
- N : a positive integer,
- $\mathcal{O}_N$: the order in K of conductor N,
- $H_{\mathcal{O}_N}$: the ring class field of the order $\mathcal{O}_N$ in K.

2. Extended form class groups

We briefly review extended form class groups, generalizing Gauss's classical form class groups, due to Jung et al [7], [8] and Shin [13].

Let $I(N\mathcal{O}_K)$ be the group of fractional ideals of K prime to $N\mathcal{O}_K$, and let $P_\mathbb{Z}(N\mathcal{O}_K)$ be its subgroup defined by

$$P_\mathbb{Z}(N\mathcal{O}_K) = \left\langle \nu\mathcal{O}_K ~\middle|~ \begin{array}{l} \nu \text{ is a nonzero element of } \mathcal{O}_K \text{ such that} \\ \nu \equiv t \pmod{N\mathcal{O}_K} \text{ for some integer } t \text{ prime to } N \end{array} \right\rangle.$$

Then, for the generalized ideal class group

$$\mathcal{C}_\mathbb{Z}(N\mathcal{O}_K) := I(N\mathcal{O}_K)/P_\mathbb{Z}(N\mathcal{O}_K),$$

we have

$$\mathcal{C}(\mathcal{O}_N) \simeq \mathcal{C}_\mathbb{Z}(N\mathcal{O}_K) \simeq \mathrm{Gal}(H_\mathcal{O}/K)$$

(see [1, Proposition 7.22 and §9.A]).

Let $\mathcal{Q}(d_K,\, N)$ be the set of certain binary quadratic forms over $\mathbb{Z}$ given by

$$\mathcal{Q}(d_K,\, N) := \left\{ ax^2 + bxy + cy^2 \in \mathbb{Z}[x,\, y] ~\middle|~ \begin{array}{l} \gcd(a,\, b,\, c) = \gcd(a,\, N) = 1, \\ b^2 - 4ac = d_K,\ a > 0 \end{array} \right\}.$$

The Hecke congruence subgroup $\Gamma_0(N)$ acts on the set $\mathcal{Q}(d_K,\,N)$ as

$$(2)\qquad Q\left(\begin{bmatrix}x\\y\end{bmatrix}\right)^{\gamma}=Q\left(\gamma\begin{bmatrix}x\\y\end{bmatrix}\right)\qquad (Q(x,\,y)\in\mathcal{Q}(d_K,\,N),\ \gamma\in\Gamma_0(N)),$$

which yields the equivalence relation $\sim_{\Gamma_0(N)}$. Let

$$\mathcal{C}_0(d_K,\,N):=\mathcal{Q}(d_K,\,N)/\sim_{\Gamma_0(N)}$$

be the corresponding set of equivalence classes. For $Q(x,\,y)=ax^2+bxy+cy^2\in\mathcal{Q}(d_K,\,N)$, recall the definition (1) of ω_Q.

Proposition 2.1. *The set $\mathcal{C}_0(d_K,\,N)$ can be equipped with a group structure so that the map*

$$\begin{aligned}\mathcal{C}_0(d_K,\,N)&\to\mathcal{C}_{\mathbb{Z}}(N\mathcal{O}_K)\\ [Q]&\mapsto[[\omega_Q,\,1]]\end{aligned}$$

becomes a well-defined isomorphism. Hence there is an isomorphism from $\mathcal{C}_0(d_K,\,N)$ onto $\mathrm{Gal}(H_{\mathcal{O}_N}/K)$.

Proof. See [13, Theorem 3.3] or [7, Theorem 5.4]. □

The group $\mathcal{C}_0(d_K,\,N)$ is called an *extended form class group* of discriminant d_K and level N.

Lemma 2.2. *The ring class field $H_{\mathcal{O}_N}$ is preserved by the complex conjugation. Thus $H_{\mathcal{O}_N}$ is a Galois extension of $\mathbb{Q}$ whose Galois group can be written as a semidirect product*

$$\mathrm{Gal}(H_{\mathcal{O}_N}/\mathbb{Q})=\mathrm{Gal}(H_{\mathcal{O}_N}/K)\rtimes\{1,\,\mathfrak{c}\},$$

where $\mathfrak{c}$ is the complex conjugation restricted to $H_{\mathcal{O}_N}$.

Proof. See [1, Lemma 9.3]. □

Remark 2.3. The action of $\mathfrak{c}$ on $\mathrm{Gal}(H_{\mathcal{O}_N}/K)$ is given by $g\mapsto g^{-1}$.

Let

$$\mathcal{Q}(d_K,\,N)^{\pm}:=\{Q,\,-Q\mid Q\in\mathcal{Q}(d_K,\,N)\}\quad(\subset\mathbb{Z}[x,\,y]).$$

The group $\Gamma_0(N)$ also acts on the set $\mathcal{Q}(d_K,\,N)^{\pm}$ in the same way as (2), and induces the equivalence relation $\sim^{\pm}_{\Gamma_0(N)}$. We obtain the corresponding set of equivalence classes

$$\mathcal{C}_0(d_K,\,N)^{\pm}:=\mathcal{Q}(d_K,\,N)^{\pm}/\sim^{\pm}_{\Gamma_0(N)}.$$

For $Q \in \mathcal{Q}(d_K,\, N)^\pm$, define

$$\mathrm{sgn}(Q) := \begin{cases} 1 & \text{if } Q \text{ is positive definite,} \\ -1 & \text{if } Q \text{ is negative definite.} \end{cases}$$

One sees that the function

$$\mathrm{sgn} : \mathcal{Q}(d_K,\, N)^\pm \to \{1,\, -1\}$$

is well defined on $\mathcal{C}_0(d_K,\, N)^\pm$.

Let

$$\phi_{K,\,N} : \mathcal{C}_0(d_K,\, N) \xrightarrow{\sim} \mathrm{Gal}(H_\mathcal{O}/K)$$

be the isomorphism stated in Proposition 2.1.

Proposition 2.4. *The map*

$$\begin{aligned} \phi^\pm_{K,\,N} : \mathcal{C}_0(d_K,\, N)^\pm &\to \mathrm{Gal}(H_{\mathcal{O}_N}/\mathbb{Q}) \\ [Q] &\mapsto \phi_{K,\,N}([\mathrm{sgn}(Q)Q])\mathfrak{c}^{\frac{1-\mathrm{sgn}(Q)}{2}} \end{aligned}$$

is well defined and is bijective, where $\mathfrak{c}$ is the complex conjugation restricted to $H_{\mathcal{O}_N}$. Hence $\mathcal{C}_0(d_K,\, N)^\pm$ can be given a group structure isomorphic to $\mathrm{Gal}(H_{\mathcal{O}_N}/\mathbb{Q})$*, having $\mathcal{C}_0(d_K,\, N)$ as its subgroup.*

Proof. The result is straightforward from Proposition 2.1 and Lemma 2.2. □

Remark 2.5. Let $Q \in \mathcal{Q}(d_K,\, N)^\pm$. Note that

$$\mathrm{sgn}(Q^\gamma) = \mathrm{sgn}(Q) \quad \text{for all } \gamma \in \Gamma_0(N).$$

Thus the notation $[Q]$ does not cause any confusion, if $[Q]$ is an element of $\mathcal{C}_0(d_K,\, N)$ or, of $\mathcal{C}_0(d_K,\, N)^\pm$.

3. Inverse limits

As usual, let $\mathbb{N}$ denote the set of positive integers. We endow the set $\mathbb{N}$ with the partial order $\preccurlyeq$ defined by divisibility: for $N,\, M \in \mathbb{N}$

$$N \preccurlyeq M \quad \Longleftrightarrow \quad N \,|\, M.$$

Then we have the directed partially ordered set $(\mathbb{N},\, \preccurlyeq)$.

Lemma 3.1. *Let $N,\, M \in \mathbb{N}$ be such that $N \preccurlyeq M$. Then the inclusion $H_{\mathcal{O}_N} \subseteq H_{\mathcal{O}_M}$ holds.*

Proof. Recall that

$$\mathcal{C}_{\mathbb{Z}}(M\mathcal{O}_K) = I(M\mathcal{O}_K)/P_{\mathbb{Z}}(M\mathcal{O}_K) \simeq \mathrm{Gal}(H_{\mathcal{O}_M}/K),$$
$$\mathcal{C}_{\mathbb{Z}}(N\mathcal{O}_K) = I(N\mathcal{O}_K)/P_{\mathbb{Z}}(N\mathcal{O}_K) \simeq \mathrm{Gal}(H_{\mathcal{O}_N}/K)$$

via the Artin maps. Consider the natural (canonical) homomorphism

$$\begin{aligned}\sigma : I(M\mathcal{O}_K) &\to I(N\mathcal{O}_K)/P_{\mathbb{Z}}(N\mathcal{O}_K)\\ \mathfrak{a} &\mapsto [\mathfrak{a}].\end{aligned}$$

Let ν be a nonzero element of $\mathcal{O}_K$ satisfying

$$\nu \equiv t \pmod{M\mathcal{O}_K} \quad \text{for some integer } t \text{ prime to } M.$$

Since $\nu \equiv t \pmod{N\mathcal{O}_K}$ and t is prime to M, the ideal $\nu\mathcal{O}_K$ belongs to the kernel of the homomorphism σ. This argument implies the inclusion

$$P_{\mathbb{Z}}(M\mathcal{O}_K) \subseteq \ker(\sigma).$$

Thus we achieve by class field theory (cf. [1, Corollary 8.7]) that $H_{\mathcal{O}_N}$ is a subfield of $H_{\mathcal{O}_M}$. □

We attain by Lemmas 2.2 and 3.1 an inverse system

$$\{\mathrm{Gal}(H_{\mathcal{O}_N}/\mathbb{Q})\}_{N\in\mathbb{N}}.$$

Here, the transition map $\mathrm{Gal}(H_{\mathcal{O}_M}/\mathbb{Q}) \to \mathrm{Gal}(H_{\mathcal{O}_N}/\mathbb{Q})$ is given by restriction for N, $M \in \mathbb{N}$ satisfying $N \preccurlyeq M$. Observe that

$$\varprojlim_{N\in\mathbb{N}} \mathrm{Gal}(H_{\mathcal{O}_N}/\mathbb{Q}) \simeq \mathrm{Gal}(K^{\mathrm{ring}}/\mathbb{Q})$$

where

$$K^{\mathrm{ring}} := \bigcup_{N\in\mathbb{N}} H_{\mathcal{O}_N}.$$

4. Inverse limits of the CM points

Now, we introduce the notion of certain CM points on the Shimura variety $Y_0(N)^{\pm}$, and prove the main theorem of the present paper on their inverse limits.

Definition 4.1. Let $\tau \in \mathbb{H} \cup \mathbb{H}^-$ be a CM point (i.e. τ is imaginary quadratic), and let $ax^2+bx+c \in \mathbb{Z}[x]$ be a primitive quadratic polynomial having τ as a root.

(i) The *discriminant* of τ is defined to be b^2-4ac, the discriminant of the polynomial ax^2+bx+c.

(ii) We say that τ is *primitive modulo* N if $\gcd(a,\, N)=1$.

We denote by $\mathbb{H}(d_K,\, N)^{\pm}$ the set of CM points in $\mathbb{H}\cup\mathbb{H}^-$ which are of discriminant d_K and are primitive modulo N.

DEFINITION 4.2. Let

$$\mathcal{CM}_0(d_K,\, N)^{\pm} := \left\{[\tau]\in Y_0(N)^{\pm} \mid \tau\in\mathbb{H}(d_K,\, N)^{\pm}\right\}.$$

We also call an element of $\mathcal{CM}_0(d_K,\, N)^{\pm}$ a *CM point* (that is of discriminant d_K and is primitive modulo N).

The next lemma is similar to [6, Lemma 3.3], and we give its proof for completeness.

LEMMA 4.3. *The map*

$$\begin{aligned}\rho : \mathcal{C}_0(d_K,\, N)^{\pm} &\to \mathcal{CM}_0(d_K,\, N)^{\pm}\\ [Q] &\mapsto \begin{cases}[\omega_Q]\ (\in Y_0(N)) & \textit{if}\ \mathrm{sgn}(Q)=1,\\ [\overline{\omega}_{-Q}]\ (\in Y_0(N)^-) & \textit{if}\ \mathrm{sgn}(Q)=-1\end{cases}\end{aligned}$$

is a well-defined bijection. Here, $\overline{\cdot}$ *means the complex conjugation.*

Proof. Let Q and Q' be two forms in $\mathcal{Q}(d_K,\, N)^{\pm}$ such that $[Q]=[Q']$ in $\mathcal{C}_0(d_K,\, N)^{\pm}$. Then we have $Q'=Q^{\gamma}$ for some $\gamma\in\Gamma_0(N)$, and so

$$-Q' = -(Q^{\gamma}) = (-Q)^{\gamma} \quad (\in\mathbb{Z}[x,\, y]).$$

Observe that

$$\begin{cases}\omega_{Q'}=\omega_{Q^{\gamma}}=\gamma^{-1}(\omega_Q) & \text{if}\ \mathrm{sgn}(Q)=1,\\ \overline{\omega}_{-Q'}=\overline{\omega}_{(-Q)^{\gamma}}=\overline{\gamma^{-1}(\omega_{-Q})}=\gamma^{-1}(\overline{\omega}_{-Q}) & \text{if}\ \mathrm{sgn}(Q)=-1.\end{cases}$$

This proves that the map ρ is well defined.

We deduce by the fact $Y_0(N) \cap Y_0(N)^- = \emptyset$ that for $Q,\, Q' \in \mathcal{Q}(d_K,\, N)^\pm$,

$$\begin{aligned}
\rho([Q]) = \rho([Q']) &\iff \begin{cases} [\omega_Q] = [\omega_{Q'}] & \text{if } \operatorname{sgn}(Q) = 1, \\ [\overline{\omega}_{-Q}] = [\overline{\omega}_{-Q'}] & \text{if } \operatorname{sgn}(Q) = -1 \end{cases} \\
&\iff \text{there is } \gamma \in \Gamma_0(N) \text{ such that} \\
&\qquad \begin{cases} \omega_Q = \gamma(\omega_{Q'}) & \text{if } \operatorname{sgn}(Q) = 1, \\ \overline{\omega}_{-Q} = \gamma(\overline{\omega}_{-Q'}) & \text{if } \operatorname{sgn}(Q) = -1 \end{cases} \\
&\iff \text{there is } \gamma \in \Gamma_0(N) \text{ such that} \\
&\qquad \begin{cases} \omega_Q = \gamma(\omega_{Q'}) & \text{if } \operatorname{sgn}(Q) = 1, \\ \omega_{-Q} = \gamma(\omega_{-Q'}) & \text{if } \operatorname{sgn}(Q) = -1 \end{cases} \\
&\iff \text{there is } \gamma \in \Gamma_0(N) \text{ such that} \\
&\qquad \begin{cases} Q' = Q^\gamma & \text{if } \operatorname{sgn}(Q) = 1, \\ -Q' = (-Q)^\gamma = -(Q^\gamma) & \text{if } \operatorname{sgn}(Q) = -1 \end{cases} \\
&\iff [Q] = [Q'] \text{ in } \mathcal{C}_0(d_K,\, N)^\pm.
\end{aligned}$$

This shows that ρ is injective.

To prove that ρ is surjective, let $\tau \in \mathbb{H}(d_K,\, N)^\pm$. Note that there is a unique form Q in $\mathcal{Q}(d_K,\, N)$ for which τ is a root of the quadratic polynomial $Q(x,\, 1)$. If we let

$$Q' = \begin{cases} Q & \text{if } \tau \in \mathbb{H}, \\ -Q & \text{if } \tau \in \mathbb{H}^-, \end{cases}$$

then we get that

$$\rho([Q']) = \begin{cases} \rho([Q]) = [\omega_Q] = [\tau] & \text{if } \tau \in \mathbb{H}, \\ \rho([-Q]) = [\overline{\omega}_Q] = [\tau] & \text{if } \tau \in \mathbb{H}^-. \end{cases}$$

Therefore ρ is surjective, and hence it is bijective. $\square$

THEOREM 4.4. *Let K be an imaginary quadratic field. Then the inverse limit*

$$\varprojlim_N \mathcal{CM}_0(d_K,\, N)^\pm \quad (\subset \varprojlim_N Y_0(N)^\pm)$$

can be regarded as a group isomorphic to the Galois group $\operatorname{Gal}(K^{\mathrm{ring}}/\mathbb{Q})$*, where K^{ring} denotes the compositum of all ring class fields $H_{\mathcal{O}_N}$.*

Proof. We derive that as a set

$$\begin{aligned}\varprojlim_N \mathcal{CM}_0(d_K,\,N)^{\pm} &\simeq \varprojlim_N \mathcal{C}_0(d_K,\,N)^{\pm} \quad \text{by Lemma 4.3}\\ &\simeq \varprojlim_N \mathrm{Gal}(H_{\mathcal{O}_N}/\mathbb{Q}) \quad \text{by Proposition 2.4}\\ &\simeq \mathrm{Gal}\left(\bigcup_N H_{\mathcal{O}_N}/\mathbb{Q}\right)\\ &= \mathrm{Gal}(K^{\mathrm{ring}}/\mathbb{Q}).\end{aligned}$$

Therefore the inverse limit $\varprojlim_N \mathcal{CM}_0(d_K,\,N)^{\pm}$ can be viewed as a group isomorphic to $\mathrm{Gal}(K^{\mathrm{ring}}/\mathbb{Q})$ via the bijection discussed above. □

Remark 4.5. Theorem 4.4 is closely related to the recent work of Jung-Koo-Shin [6].

5. Galois actions on special values of modular functions

In this final section, we describe the Galois action of the inverse limit $\varprojlim_N \mathcal{C}_0(d_K,\,N)^{\pm}$ in an explicit way.

Let $\mathcal{F}_{0,\,N}(\mathbb{Q})$ be the field of meromorphic modular functions for $\Gamma_0(N)$ with rational Fourier coefficients. Then,

$$\mathcal{F}_{0,\,N}(\mathbb{Q}) = \mathbb{Q}\left(j,\, j\circ\begin{bmatrix}N & 0\\ 0 & 1\end{bmatrix}\right)$$

where j is the elliptic modular function (see [1, Theorem 11.9] and [9, Lemma 4.1]). Define an element τ_K of $K\cap\mathbb{H}$ by

$$\tau_K := \begin{cases}\frac{-1+\sqrt{d_K}}{2} & \text{if } d_K\equiv 1 \pmod 4,\\ \frac{\sqrt{d_K}}{2} & \text{if } d_K\equiv 0 \pmod 4,\end{cases}$$

and so $\mathcal{O}_K = [\tau_K,\,1]$. By the theory of canonical models for modular curves due to Shimura [12], we have

$$H_{\mathcal{O}_N} = K\left(f(\tau_K)\mid f\in\mathcal{F}_{0,\,N}(\mathbb{Q}) \text{ is finite at } \tau_K\right)$$

(see [10, Theorem 3.4]).

Proposition 5.1. *Let $Q\in\mathcal{Q}(d_K,\,N)$, and let $f\in\mathcal{F}_{0,\,N}(\mathbb{Q})$ be finite at τ_K. Then we have*

$$f(\tau_K)^{\phi_{K,\,N}([Q])} = f(-\overline{\omega}_Q).$$

Proof. See [8, Theorem 12.3] and Proposition 2.4. □

For $Q \in \mathcal{Q}(d_K,\, N)^{\pm}$, we further adopt the notation $[Q]_N$ for the class of Q in $\mathcal{C}_0(d_K,\, N)^{\pm}$.

Proposition 5.2. *Let*

$$s = ([Q_1]_1,\, [Q_2]_2,\, [Q_3]_3,\, \ldots) \;\in\; \varprojlim_{N} \mathcal{C}_0(d_K,\, N)^{\pm}$$

for some $Q_N \in \mathcal{Q}(d_K,\, N)^{\pm}$ $(N = 1,\, 2,\, 3,\, \ldots)$. *We consider* s *as a Galois element in* $\mathrm{Gal}(K^{\mathrm{ring}}/\mathbb{Q})$ *in view of* Theorem 4.4.

(i) *We have*

$$\tau_K^s = \begin{cases} \tau_K & \text{if } \mathrm{sgn}(Q_1) = 1, \\ \overline{\tau}_K & \text{if } \mathrm{sgn}(Q_1) = -1. \end{cases}$$

(ii) *If* $f \in \mathcal{F}_{0,\,N}(\mathbb{Q})$ *is finite at* τ_K, *then we get that*

$$f(\tau_K)^s = \begin{cases} f(-\overline{\omega}_Q) & \text{if } \mathrm{sgn}(Q_1) = 1, \\ \overline{f(-\overline{\omega}_{-Q})} & \text{if } \mathrm{sgn}(Q_1) = -1. \end{cases}$$

Proof. The result is a consequence of Propositions 2.4 and 5.1. □

References

[1] D. A. Cox, *Primes of the Form $x^2 + ny^2$–Fermat, Class field theory, and Complex Multiplication*, 3rd ed. with solutions, with contributions by Roger Lipsett, AMS Chelsea Publishing, Providence, R.I., 2022.

[2] H. Hasse, *Neue Begründung der Komplexen Multiplikation I, II*, J. Reine Angew. Math. 157, 165 (1927, 1931), 115–139, 64–88.

[3] M. Deuring, *Die Klassenkörper der komplexen Multiplikation*, Enzyklopädie der mathematischen Wissenschaften: Mit Einschluss ihrer Anwendungen, Band I 2, Heft 10, Teil II (Article I 2, 23), B. G. Teubner Verlagsgesellschaft, Stuttgart, 1958.

[4] C. F. Gauss, *Disquisitiones Arithmeticae*, Leipzig, 1801.

[5] G. J. Janusz, *Algebraic Number Fields*, 2nd ed., Grad. Studies in Math. 7, Amer. Math. Soc., Providence, R.I., 1996.

[6] H. Y. Jung, J. K. Koo and D. H. Shin, *Inverse limits of CM points on certain Shimura varieties*, Expo. Math. 44 (2026), no. 2, 1–13.

[7] H. Y. Jung, J. K. Koo, D. H. Shin and D. S. Yoon, *Class fields and form class groups for solving certain quadratic Diophantine equations*, J. Number Theory 275 (2025), 1–34.

[8] H. Y. Jung, J. K. Koo, D. H. Shin and D. S. Yoon, *Arithmetic properties of orders in imaginary quadratic fields*, Indian J. Pure Appl. Math., published online 2025, https://doi.org/10.1007/s13226-025-00801-w.

[9] J. K. Koo and D. H. Shin, *On some arithmetic properties of Siegel functions*, Math. Zeit. 264 (2010), no. 1, 137–177.

[10] J. K. Koo and D. H. Shin, *Singular values of principal moduli*, J. Number Theory 133 (2013) no. 2, 475–483.

[11] J. Neukirch, *Class Field Theory*, Grundlehren der Mathematischen Wissenschaften 280, Springer-Verlag, Berlin, 1986.

[12] G. Shimura, *Introduction to the Arithmetic Theory of Automorphic Functions*, Iwanami Shoten and Princeton University Press, Princeton, N.J., 1971.

[13] D. H. Shin, *Binary quadratic forms and ring class fields*, J. Basic Sci. HUFS **45** (2018), pp. 1–10.

6. Author Information

Dong Hwa Shin (dhshin@hufs.ac.kr)
Professor, Department of Mathematics, Hankuk University of Foreign Studies, South Korea.

J. Basic Sci., HUFS, **61** (2026), pp. 19-23

Nano bubble electrical properties[1]

Taekyeong Kim[2]

Introduction

Here, we report ε measurements for nanoscale bubbles of MoS_2 by probing the polarization forces under an applied electric field oscillating at low frequency based on electrostatic force microscopy (EFM). Remarkably, regardless of the bubble size, such as height and radius, the higher ε of 6~8 are observed for the bubbles of MoS_2 as compared to flat regions with the value of ~3. We find that the charge carrier increase owing to the strain-induced band gap reduction which is independent of the bubbles' height or radius is responsible for the enhanced ε of the bubbles of MoS_2, in agreement with our calculations based on the Clausius-Mossotti relation.

Experimental

In order to find the for a nanobubble based on the measured dC/dz signals, we employ finite-element calculations considering the exact geometrical parameters in our experiments, such as tip and nanobubble structures on graphite substrate. It is well known that the water molecules are trapped in nanobubbles due to the vdW interaction between MoS_2 and graphite surface in the process of MoS_2 transfer onto graphite flake, and the confined water at the nanoscale has its own dielectric constant depending on the water thickness. Our three-dimensional (3D) electrostatic model takes into account the specific geometry of a nanobubble as the core-shell structure which consist of the curved MoS_2 and the confined water inside a nanobubble for the dC/dz curve calculation, as reported in literature (. Figure 1 shows the calculated dC/dz (lines) as a function of κ (fitting parameter) for the known geometries of the nanobubble (red) and the flat (blue). Based on the measured z, and h values.

---

[1] This research was supported by the research fund 2025 of Hankuk University of Foreign Studies.
[2] Department of Physics, Hankuk University of Foreign Studies, Yongin 17035, Republic of Korea. E-mail: tkim@hufs.ac.kr

Results and Discussion

In order to elucidate the enhanced and their size independent behavior of the nanobubbles, we employ the modified Clausius-Mossotti relation for a 2D atomic crystal, as reported in literature. Figure1 contrasts the EF-hysteresis curves measured on a flat region (red) and a nanobubble with a height of ~8 nm (blue) of few-layer MoS_2 on a SiO_2/Si substrate when VG is swept from -35 V to 10 V (forward) and back to -35 V (backward) at a sweep rate of 0.16 Hz. After acquiring each EF-hysteresis curve, VG is set to -35 V for a few seconds to ensure that the MoS_2 recovers fully from the previous VG stress. The unscreened electric field from the back gate in the bare SiO_2 region can affect VCPD due to the long-range electrostatic interaction between the conducting cantilever and the back gate during the VG sweep process. Because the surface potential of an Au metal electrode is not affected by VG due to the high density of states near the Fermi energy of Au metal, the background.

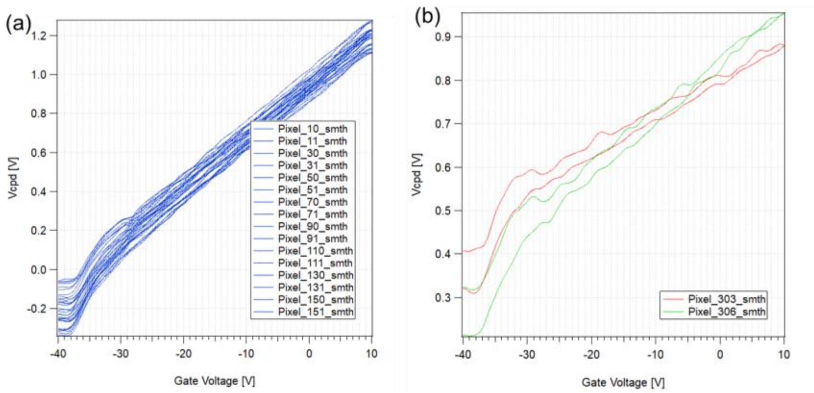

Figure 1. EF-hysteresis curves depending on the VG sweep range. EF-hysteresis curves on a flat region (a) and a nanobubble (b) with the maximum positive VG (VG,max) being gradually increased from 2 V to 16 V while the negative minimum VG is fixed at -40 V during the sweeping of VG. The sweep rates are 0.16 Hz for all EF-hysteresis measurements. The EF levels are pinned near the EC of MoS_2 at VG of -20 V due to the high concentration of electrons and remain there as VG increases.

The lower oxide trap band is located near the MoS_2 valence band edge (EV) and does not have a considerable impact on the hysteresis in MoS_2 FETs because the EF of MoS_2 shifts in the upper half of the band gap during the VG sweeps process. Therefore, we only consider the upper oxide trap band for the charge trapping and EF-hysteresis. The upper oxide trap band is assumed to be an acceptor-type trap which is negatively charged below the EF and neutral above the EF of MoS27. Given that the oxide traps exchange the charge with the MoS_2 channel through the tunneling process, these traps should be located within a few nanometers from the MoS_2/SiO_2 interface. We use dox = 2 nm as the maximum distance of the active oxide traps from the interface. It is well known that H_2O and hydrocarbon molecules are trapped in nanobubbles that form inevitably during the MoS_2 stacking process. We simply assume that 100% of the H_2O or hydrocarbon molecules are trapped in the nanobubble, leading to an additional dielectric layer between the MoS_2 and SiO_2 in the energy bands of the nanobubble. Based on this understanding of the energy band diagrams with the oxide traps, we will characterize quantitatively the dependence of EF-hysteresis on the height of a nanobubble. Figure 2 shows the high-resolution image of EF-hysteresis, that is, a V image of a single nanobubble, where V is measured at an EF of 0.65 eV.

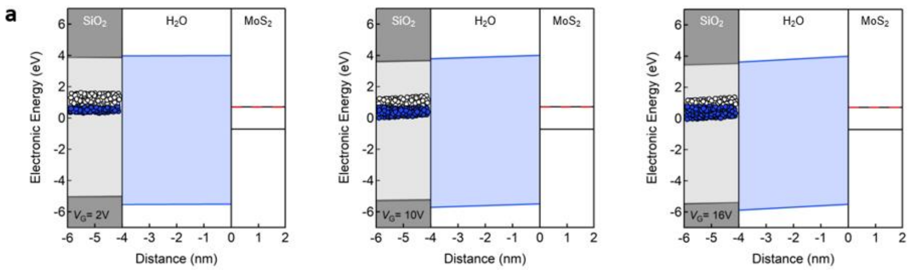

Figure 2. Calculation of the VG,max dependent V. Energy band diagrams of a nanobubble with a 4-nm-thick H_2O dielectric layer for VG,max = 2 V, 10 V, and 16 V, as examples.

The inset is the corresponding topography image of the nanobubble, showing a peak height of 8.5 nm. We observe a non-uniform V by obtaining spatially resolved EF-hysteresis curves of the nanobubble, where the maximum V occurs at its apex. It exhibits four distinct EF-hysteresis curves measured on flat and nanobubble regions with different heights of 1.8 nm, 4 nm, and 6.7 nm of the nanobubble, as denoted by the circles. This figure clearly shows that the regions with higher heights correspond to larger V values in the EF-hysteresis image and curves of the nanobubble.

The energy-level alignment of oxide traps with MoS_2 EF under gate sweeps causes hysteresis in the transfer characteristics of the conventional MoS_2 FETs, whereas the additional downward bending of the oxide trap band in conjunction with the band of the H_2O dielectric layer at a positive VG leads to an increased number of occupied charge traps below the MoS_2 EF and enlarged EF- and IDS -hysteresis in a nanobubble. The trap densities extracted from the measured EF-hysteresis curves of flat and nanobubble regions are well described by the oxide trap band model, which further confirms that the EF-hysteresis originates from the oxide traps and our band bending scenario is essential for local charge tapping/detrapping in nanobubble structures.

Acknowledgements

이 연구는 2025년 한국외국어대학교 학술연구비 지원에 의해 이루어진 것임.

References

[1] Akinwande D, et al. Graphene and two-dimensional materials for silicon technology. Nature 573, 507-518 (2019).

[2] Huo N, Konstantatos G. Recent Progress and Future Prospects of 2D-Based Photodetectors. Adv. Mater. 30, e1801164 (2018).

[3] Migliato Marega G, et al. Logic-in-memory based on an atomically thin semiconductor. Nature 587, 72-77 (2020).

[4] Nalwa HS. A review of molybdenum disulfide (MoS_2) based photodetectors: from ultra-broadband, self-powered to flexible devices. RSC Adv. 10, 30529-30602 (2020).

[5] Jiang J, et al. Flexo-photovoltaic effect in MoS_2. Nat. Nanotechnol. 16, 894-901 (2021).

[6] Manzeli S, Dumcenco D, Migliato Marega G, Kis A. Self-sensing, tunable monolayer MoS_2 nanoelectromechanical resonators. Nat. Commun. 10, 4831 (2019).

[7] Illarionov YY, et al. Insulators for 2D nanoelectronics: the gap to bridge. Nat. Commun. 11, 3385 (2020).

[8] Li T, Du G, Zhang B, Zeng Z. Scaling behavior of hysteresis in multilayer MoS_2 field effect transistors. Appl. Phys. Lett. 105, 093107 (2014).

저자정보

주저자: 김태경 / 한국외국어대학교 전자물리학과 / 교수

J. Basic Sci., HUFS, **61** (2026), pp. 24-30

지하철 네트워크 기반의 상업시설의 위치 선정[1]

유세기[2]

지하철은 도시에서 정시성이라는 특징으로 인해 주요한 대중 교통 수단이며, 시내에 존재하는 상업 시설은 역세권이라고 하는 지하철 네트워크 상에 있는 역의 영향을 지대하게 받을 수밖에 없다. 서울시 전체 지하철역을 중심으로 원의 반지름을 변화시는 탐색 방법으로, 스타벅스 커피 상점과 붕어빵 판매점의 공간 분포를 정량적으로 분석하였다. 전체적으로 붕어빵 판매점이 스타벅스보다 2.6배 많음에도 불구하고, 시내의 주요 허브 역 주변에서는 스타벅스가 매우 우세하며, 이는 지하철 네트워크의 위상학적 중심성이 상업 입지 선택에 결정적 영향을 미침을 보여준다. 본 연구는 복잡계 물리학의 관점에서 도시 교통 네트워크와 상업 생태계 간의 상호작용을 규명하였으며, 제시된 방법론은 다양한 업종과 도시권 그리고 시간적 변화에도 적용될 수 있다.

서 론

현대의 도시는 복잡한 교통 네트워크를 포함하고 있는 대표적인 복잡계(complex system)로 볼 수 있다. 이러한 대도시권에서 지하철은 정시성, 대량 수송 능력, 그리고 기후 조건에 대한 독립성으로 인해 가장 중요한 대중교통 수단으로 자리잡았으며, 도시 내 인구 이동의 중추적인 역할을 담당하고 있다. 이러한 지하철 네트워크는 단순한 교통 인프라를 넘어 도시 공간 구조의 형성과 경제 활동의 분포에 결정적인 영향을 미치는 핵심 요소로 작용한다. 도시 내 상업 시설의 입지 선택은 다양한 요인에 의해 영향을 받지만, 그 중에서도 접근성(accessibility)과 유동인구는 가장 중요한 결정 요인으로 알려져 있다. 지하철역 주변의 역세권은 유동인구가 많고 대중교통 접근성이 좋기 때문에, 상업 시설이 자연스럽게 집중되는 경향을 보인다. 이러한 현상은 공간 통계학(spatial statistics)을 비롯한 도시 경제학 분야에서 오랫동안

[1] This research was supported by the research fund 2025 of Hankuk University of Foreign Studies.
[2] Department of Physics, Hankuk University of Foreign Studies, Yongin 17035, Republic of Korea. E-mail: segiyu@hufs.ac.kr

연구되어 왔으나, 최근에는 복잡계 물리학 및 네트워크 과학(network science)의 관점에서 새로운 해석이 시도되고 있다. 특히 지하철 네트워크는small-world 특성을 가진 복잡 네트워크로 분석되며, 환승역과 같은 허브(hub) 노드가 네트워크 전체의 연결성과 효율성에 핵심적인 역할을 수행한다는 것이 다수의 연구를 통해 밝혀졌다 [1-4].

상업적 시설의 공간 분포와 교통 네트워크 간의 상관관계를 이해하는 것은 단순히 학술적 관심사를 넘어 도시 계획, 상권 분석, 그리고 지속가능한 도시 개발에 실용적인 시사점을 제공한다. 기존 연구들은 주로 집계된 통계 자료나 제한된 샘플링을 통해 이루어져 왔으며, 실제 상점 위치 데이터를 활용한 대규모 공간 분석은 상대적으로 부족한 실정이다. 또한 상점의 업종에 따라 지하철 네트워크에 대한 의존도나 공간 분포 패턴이 상이할 수 있으나, 이에 대한 비교 연구 역시 제한적이었다. 본 연구에서는 서울시를 대상으로 두 가지 상이한 특성을 가진 상업 시설—글로벌 프랜차이즈 커피 체인인 스타벅스와 전통적 노점 형태의 붕어빵 판매점—의 공간 분포를 분석하고, 지하철 역을 중심으로 한 원 안에 있는 점포 숫자를 계량적으로 측정하여 이들이 지하철 네트워크와 어떠한 상관관계를 나타내는지 정량적으로 규명하고자 한다. 스타벅스는 고정된 상업 공간을 필요로 하며 상대적으로 높은 임대료를 감당할 수 있는 대형 프랜차이즈의 전형적인 사례이며, 붕어빵 판매점은 계절성과 이동성을 가진 소규모 상업 활동의 대표적인 형태이다. 이 두 업종의 비교 분석을 통해 상업 시설의 특성에 따른 지하철 네트워크 의존도의 차이를 밝히고자 하며, 여기에서 제시한 방법론이 다른 분야로도 쉽게 응용 가능함을 보이고자 한다.

지하철역 중심 상점 분포의 공간 분석 방법

서울시 지하철 네트워크 상의 역 주위에 존재하는 상점이 어떻게 분포하는 지에 관한 공간적 상관관계(spatial correlation)를 정량적으로 규명하기 위해

지하철역을 중심으로 상점의 분포를 파악하고자 한다. 주어진 지하철역을 중심으로 반지름이 r인 원을 그림 1과 같이 그린다. 해당 원 안에 존재하는 상점의 개수를 세고, 원의 반지름을 변화시키면서(그림 1에서는 500, 1000, 1500 m로 증가) 상점의 개수를 다시 센다. 그림 1에서는, 이 지하철역을 중심으로 반지름 500, 1000, 1500 m의 동심원을 예시로 표시하였으며, 해당 영역 내에 포함되는 상점(빨간색 또는 녹색 점)의 개수가 반지름 증가에 따라 확대되는 양상을 확인할 수 있다. 이와 같이 서울시 안에 있는 모든 지하철역에 대해서 원을 이동시키며 원 안에 위치한 상점의 수를 센다. 이를 수식으로 표시하면, *i*−th 지하철역을 중심으로 반지름 r인 원 내부에 존재하는 상점의 수는 $N_i(r)$로 나타내고, 지하철 역을 따라 움직이거나(i 변화) 반지름 r을 변화시킬 수 있다. 모든 i에 대하여 합을 하게 되면 분포도 $P(N_i(r))$을 얻을 수 있게되며, 이는 서울시에 있는 모든 지하철역 주변 상점의 밀집도를 표시할 수 있는 통계적 특성으로 활용될 수 있다.

스타벅스와 붕어빵 판매점의 상대적 공간 분포

그림 2는 서울시 전체 지하철역을 대상으로 각 역을 중심으로 한 원 안에 존재하는 스타벅스 매장 수(x축)와 붕어빵 판매점 수(y축)를 나타낸 산점도(scatter plot)이다. 원의 반지름은 100부터 1500 m까지 변화시켰으며, 각 점은 특정 지하철역과 특정 반지름에 해당하는 데이터를 나타낸다. 점의 색상은 탐색 영역의 반지름을 의미하며, 밝은 색(회색)은 작은 반지름(100−300 m), 어두운 색(검정색)은 큰 반지름(1200−1500 m)에 해당한다. 전체적으로 서울시 내 붕어빵 판매점의 총 개수는 스타벅스 매장 수보다 약 2.6배 많다. 이는 붕어빵이 소자본의 계절성 노점 형태라는 특성을 반영한다. 그러나 그림 2의 점 분포를 살펴보면, 개별 지하철역 중심의 국지적 분석에서는 이와 상이한 양상이 관찰된다. 상당수의 점들이 y = x 선(스타벅스와 붕어빵 개수가 동일한

경우)보다 아래쪽에 위치하고 있으며, 이는 특정 지하철역 주변에서는 스타벅스 매장 수가 붕어빵 판매점보다 많다는 것을 의미한다. 특히 주목할 만한 점은 x축 값이 20-60 범위에 이르는 지하철역들이 존재한다는 것이다. 이러한 역들은 주로 서울의 주요 상권 허브에 해당하며, 반지름 1000 m 이상의 탐색 영역에서 50개 이상의 스타벅스 매장을 포함한다. 반면 동일한 역 주변의 붕어빵 판매점 수는 상대적으로 제한적이어서, 최대 60개를 넘지 않는다. 이는 프랜차이즈 커피 체인과 노점의 입지 전략이 근본적으로 다름을 의미한다. 점들의 수직 방향 분포를 분석하면, 붕어빵 판매점이 밀집된 역(y축 값 40-60)의 경우에도 스타벅스 매장 수는 상대적으로 적은(x축 값 10-30) 경우가 다수 관찰된다. 이는 붕어빵 노점은 주거 밀집 지역이나 학교 주변과 같이 일상적 보행 유동이 많은 지역에 집중되는 반면, 스타벅스는 상업 지구나 대형 상권과 같이 상업적 활동이 활발한 지역을 더 선호한다고 해석할 수 있다.

색상 분포를 통해 반지름 효과를 살펴보면, 반지름이 큰 원 안에 있는 점(어두운 색)의 경우 x, y 축 모두에서 크게 분산되어 있다. 이는 원의 반지름을 넓혀서 탐색 영역이 증가할수록 포함되는 상점 수가 당연히 증가함을 보여준다. 그러나 흥미롭게도, 동일한 반지름에서도 지하철역에 따라 상점 개수의 편차가 매우 크게 나타난다. 예를 들어, 반지름 1500 m(가장 어두운 색)의 경우, 스타벅스 개수는 역에 따라 5 개 미만부터 60 개 이상까지 10 배 이상의 차이를 보이며, 이는 지하철역의 위상학적 중요도와 주변 상권 특성이 상점 분포에 결정적 영향을 미침을 의미한다. 또한, 점들의 전체적인 분포 형태는 대략 삼각형 또는 부채꼴 모양을 형성하고 있으며, 이는 두 변수 간에 양의 상관관계가 존재하기는 하나 완전한 선형 관계는 아님을 의미한다. 스타벅스가 많은 역은 대체로 붕어빵 상점도 많은 경향이 있으나, 그 비율은 역마다 상이하며, 특히 고밀도 상권(스타벅스 30 개 이상)에서는 붕어빵 대비 스타벅스의 우세가 더욱 두드러진다. 이러한 패턴은 도시 상업 생태계가 단순히 인구 밀도나

유동인구에만 의존하는 것이 아니라, 상권이 어떠한 특성을 가지는지, 소득 수준, 소비 패턴 등 다층적 요인에 의해 영향을 받는다는 점을 시사한다.

결 론

서울시 지하철 네트워크와 상업 시설 분포 간의 공간적 상관관계를 복잡계 물리학의 관점에서 두 가지 상이한 특성을 가진 상업 시설—글로벌 프랜차이즈인 스타벅스와 전통적 노점 형태의 붕어빵 판매점—을 대상으로 지하철역 중심의 원형 탐색 영역 분석을 수행하였다. 붕어빵 노점상의 개수가 스타벅스 매장보다 많음에도 불구하고, 개별 지하철역 수준에서는 스타벅스가 더 많이 분포하는 역들이 상당수 존재함을 확인하였다. 이는 상업 시설의 입지 선택이 지하철역의 위상학적 특성과 주변 상권의 성격에 크게 영향을 받음을 의미한다. 특히 주요 허브역 주변에서는 스타벅스의 집중도가 현저히 높게 나타났으며, 이는 대형 프랜차이즈가 고밀도 상권을 선호함을 반영한다. 탐색 영역의 반지름을 변화시킨 경우에는, 동일한 공간 스케일에서도 지하철역에 따라 상점 개수의 편차가 매우 크게 나타났으며, 이는 소수의 허브 노드가 네트워크 전체의 연결성과 유동인구 집중에 지배적인 영향을 미친다는 기존 복잡 네트워크 이론과 일치한다. 본 연구에서 제시한 방법론은 향후 다양한 업종의 상업 시설 분포 연구, 그리고 시간적 변화에 따른 상권의 변화에도 확장 적용될 수 있다. 추후에 지하철역의 네트워크 중심성(centrality) 지표를 적용하면 상점 분포와 정량적인 상관관계도 도출할 수 있을 것이다.

Acknowledgements
이 연구는 2025년 한국외국어대학교 학술연구비 지원에 의해 이루어진 것임.

참고문헌

[1] Derrible, S., & Kennedy, C. (2010). The complexity and robustness of metro networks. Physica A: Statistical Mechanics and its Applications, 389(17), 3678-3691.

[2] Derrible, S. (2012). Network centrality of metro systems. PLoS ONE, 7(7), e40575.

[3] Wu, X., Dong, H., Tse, C. K., Ho, I. W. H., & Lau, F. C. M. (2017). Analysis of metro network performance from a complex network perspective. Physica A: Statistical Mechanics and its Applications, 492, 553-563.

[4] Ding, R., Ujang, N., Hamid, H. B., Manan, M. S. A., Li, R., & Wu, J. (2019). The Complex Network Theory-Based Urban Land-Use and Transport Interaction Studies. Complexity, 2019, Article ID 4180890.

저자정보

주저자: 유세기 / 한국외국어대학교 전자물리학과 / 교수

교신저자 : 유세기 / 한국외국어대학교 전자물리학과 / 교수

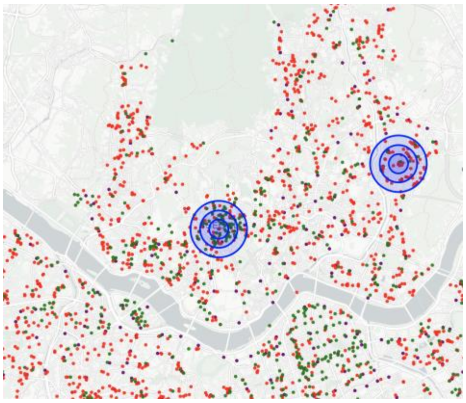

그림 1. 주어진 지하철 역을 기준으로 원을 그리고 그 안에 있는 상점의 개수를 세는 개략도. 원의 반지름을 변화시키면서(동심원 3 개는 반지름이 500, 1000, 1500 m 이다) 그 안의 상점의 개수를 셀 수도 있다. 한 역에 대하여 상점의 개수를 센 후, 서울시 안의 다른 모든 역으로 원을 옮겨가면서 상점의 개수를 세면 된다. 보라색은 지하철 역, 녹색은 스타벅스, 빨간색 점은 붕어빵 상점을 나타내고 있다.

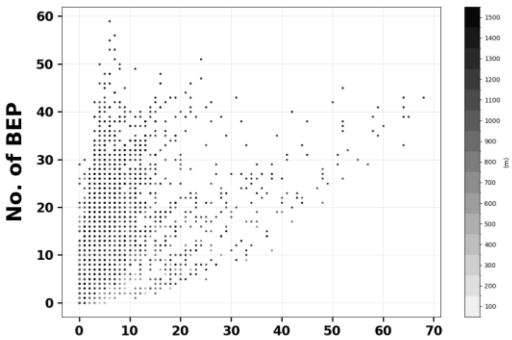

그림 2. 원의 반지름을 100 m 에서 1500 m 까지 변화시키면서 서울시 안에 있는 모든 지하철 역을 기준으로 스타벅스와 붕어빵 상점의 개수를 세서 표시한 산점도 그래프. 점은 지하철 역을 나타내고, 그 때의 x 와 y 값은 스타벅스와 붕어빵 점포의 개수를 나타내며, 원의 반지름의 크기는 색깔로 나타내면 오른쪽에 해당되는 반지름을 나타내는 자가 있다.

기초과학연구 제 61 집

인쇄 2026년 1월 30일
발행 2026년 2월 2일

발 행 인 소장 허 성
운영위원 김태경, 김해조, 명희준, 이현주, 최영수
인 쇄 처 외대문화사
발 행 소 한국외국어대학교 기초과학연구소
주 소 경기도 용인시 처인구 모현읍 외대로 81
17035

ISSN 2713-7465